Stem Cell Research 80 (2024) 103497

Contents lists available at ScienceDirect

Stem Cell Research

journal homepage: www.elsevier.com/locate/scr

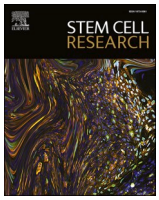

Lab Resource: Multiple Cell Lines

Generation of human induced pluripotent stem cell (hiPSC) lines derived from three patients carrying the pathogenic *CRYAB* (A527G) mutation and one non-carrier family member

Ilse R. Kelters [a,b], Devin Verbueken [c,d], Tess Beekink [a], Linda W. Van Laake [b], Joost P.G. Sluijter [a,b], Renee G.C. Maas [a,b,*], Jan W. Buikema [c,d,*]

[a] *Utrecht Regenerative Medicine Center, Circulatory Health Laboratory, University Utrecht, Department of Cardiology, University Medical Center Utrecht, 3508 GA Utrecht, the Netherlands*

[b] *Experimental Cardiology Laboratory, Department of Heart & Lungs, University Medical Center Utrecht, Heidelberglaan 100, 3584 CX Utrecht, the Netherlands*

[c] *Amsterdam Cardiovascular Sciences, Department of Physiology, VU University, Amsterdam University Medical Center, De Boelelaan 1108, 1081 HZ Amsterdam, the Netherlands*

[d] *Amsterdam Heart Center, Department of Cardiology, Amsterdam University Medical Centers, De Boelelaan 1117, 1081 HZ Amsterdam, the Netherlands*

A B S T R A C T

A newly identified pathogenic variant (A527G) in alpha B-crystallin (αB-crystallin) has been linked to congenital cataract and young-onset dilated cardiomyopathy (DCM) within a Dutch family, although the disease mechanism remains unclear. Four human induced pluripotent stem cell (hiPSC) clones were generated from three symptomatic patients carrying the A527G variant, and one healthy proband. Peripheral blood mononuclear cells (PBMCs) were reprogrammed using integration-free Sendai viral pluripotency vectors. The established hiPSCs clones exhibited regular ESC-like morphology, expression of pluripotency markers, and normal karyotyping. These hiPSC lines can facilitate future studies to understand the chaperone function and its role in DCM disease progression.

Resource Table

Unique stem cell lines identifier	UMCUi001-A UMCUi002-A UMCUi003-A UMCUi004-A
Alternative name(s) of stem cell lines	CRYAB-A527G-11C1 (11C1) CRYAB-A527G-12C6 (12C6) CRYAB-A527G-91C10 (91C10) CRYAB-A527G-92C25 (92C25)
Institution	University Medical Center Utrecht, Department of Heart & Lungs, Experimental Cardiology Laboratory
Contact information of distributor	j.sluijter@umcutrecht.nl and j.w.buikema@amsterdamumc.nl
Type of cell lines	hiPSC
Origin	Human
Additional origin info required	11C1 – Female – Age 55 – Index Patient 12C6 – Male – Age 21 – Dizygotic twin 91C10 – Male – Age 21 – Dizygotic twin 92C25 – Female – Age 23 – Healthy proband Caucasian race

(*continued on next column*)

Resource Table (*continued*)

Cell Source	Total PBMCs
Clonality	Clonal
Method of reprogramming	Sendai virus reprogramming (KOS, hcMYC and hKLF-4)
Genetic Modification	Yes
Type of Genetic Modification	Hereditary/spontaneous/naturally
Evidence of the reprogramming transgene loss (including genomic copy if applicable)	RT-/q-PCR
Associated disease	Dilated cardiomyopathy, congenital posterior polar cataract
Gene/locus	CRYAB/11q23.1 c.527A>G p.*176Trp+19
Date archived/stock date	11/2022
Cell line repository/bank	N/A
Ethical approval	Medical Ethical Committee (TCBio) of University Medical Center (UMC) Utrecht; approval number: 12-387

* Corresponding authors at: Utrecht Regenerative Medicine Center, Circulatory Health Laboratory, University Utrecht, Department of Cardiology, University Medical Center Utrecht, 3508 GA Utrecht, the Netherlands (R.G.C. Maas). Amsterdam Cardiovascular Sciences, Department of Physiology, VU University, Amsterdam University Medical Center, De Boelelaan 1108, 1081 HZ Amsterdam, the Netherlands (J.W. Buikema).

E-mail addresses: j.sluijter@umcutrecht.nl (J.P.G. Sluijter), r.g.c.maas-4@umcutrecht.nl (R.G.C. Maas), j.w.buikema@amsterdamumc.nl (J.W. Buikema).

https://doi.org/10.1016/j.scr.2024.103497
Received 1 July 2024; Accepted 11 July 2024
Available online 24 July 2024

1. Resource utility

αB-crystallin is an essential molecular chaperone that preserves proteostasis and negatively regulates apoptosis (Cheng et al., 2023; Mitra et al., 2013). The generation of human induced pluripotent stem cell (hiPSC) lines of three patients carrying a pathogenic *CRYAB* A527G mutation and their healthy proband will allow future studies on αB-crystallins function in various diseases.

2. Resource details

αB-crystallin (alternative name: HSPB5), encoded by the *CRYAB* gene, is a member of the small heat shock family. αB-crystallin acts as an ATP-independent chaperone by preventing misfolded proteins from aggregating in exposure to stress situations, moreover it contributes to intracellular architecture and inhibits apoptosis (Mitra et al., 2013). Various tumors overexpress αB-crystallin to enhance these protective properties, resulting in tumorigenesis, pro-metastatic tumor capacity, and therapy resistance (Cheng et al., 2023). Under physiological conditions, αB-crystallin is mostly expressed in the eye lens, skeletal muscle, and cardiac tissue. Consequently, *CRYAB* variants display diverse combined phenotypes, from cataracts, skeletal- and myofibrillar myopathies, to cardiomyopathies (Marcos et al., 2020).

One rare variant is the non-stop mutation at position 527, replacing the stop codon with tryptophan (A527G) resulting in continued translation of 19 extra amino acids (p.*176trp+19). *CRYAB* A527G has been shown to increase the risk of developing congenital posterior polar cataract and dilated cardiomyopathy (DCM) presenting with contractile dysfunction and heart failure at early adolescent age (van der Smagt et al., 2014). Unfortunately, current medical treatment options lack the specificity to stop disease progression and are only for symptomatic relief purposes. Currently, implantation of a left ventricular assist device or heart transplant forms the only cardiac treatment options for end-stage heart failure, although few patients are eligible for this intervention due to the low availability of donor hearts and poor patient conditions at that stage of the disease.

The development of transgenic mouse models yielded insights into the pathomechanism of *CRYAB* R120G cardiomyopathy, including abnormal desmin aggregation leading to myofibril misalignment, and abnormal mitochondrial respiration and dynamics (Alam et al., 2020). The broad range of *CRYAB* variants following a variety of clinical phenotypes, however, impedes the comparison between the pathomechanisms of the different disease-causing genotypes (Marcos et al., 2020). Here, we describe the generation of three hiPSC lines of three individual patients carrying the *CRYAB* A527G mutation and one healthy proband (Fig. 1A). Our findings will be useful for future research to resolve the underlying pathways involved in the development and progression of distinct clinical phenotypes caused by *CRYAB* mutations such as cataracts and young onset DCM.

Peripheral blood mononuclear cells (PBMCs) were reprogrammed using the CytoTune-iPS 2.0 Sendai virus reprogramming system. Two weeks after transduction, the hiPSC lines showed a typical hiPSC morphology, forming compact, well demarcated colonies with a high nuclear to cytoplasm ratio (Fig. 1B). The pluripotency of the hiPSC lines was confirmed with a positive immunostaining for the pluripotency markers OCT3/4, SOX2, TRA-1–60, and SSEA (Fig. 1B), and robust expression of pluripotency genes OCT3/4, cMYC, KLF4, NANOG, ZFP42 using RT-qPCR (Fig. 1C). Sanger Sequencing of *CRYAB* verified the presence of the heterozygotic variant in the three patients and absence in the healthy proband (Fig. 1D). All hiPSC lines showed differentiation capacity towards the three germ layers as assessed by trilineage differentiation and immunofluorescence staining (Fig. 1E). Genomic stability was confirmed by digital karyotyping (Fig. S1A-D). Short tandem repeats (STR) analysis on 17 loci excluded cell line cross-contamination (Available upon request). Mycoplasma tests in these hiPSC lines showed negative results (Fig. S1E).

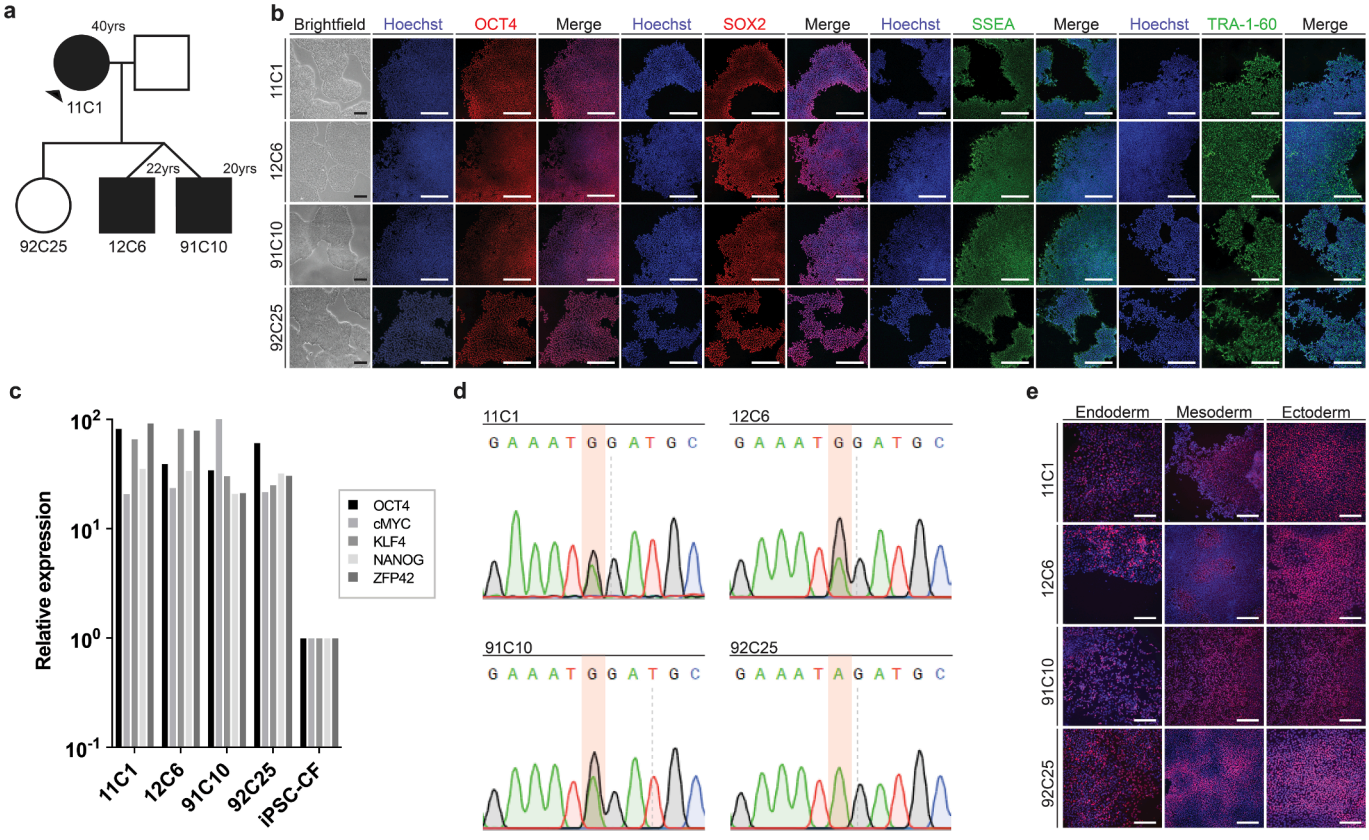

Fig. 1. Evaluation of pluripotency and differentiation potential of generated hiPSC lines.

3. Materials and methods

3.1. Reprogramming and hiPSC maintenance

Human PBMCs were collected, isolated, and cultured for 3 days before reprogramming using the Cytotune 2.0 Sendai Virus Kit (Thermofisher Scientific) at the appropriate MOI (i.e., KOS MOI=5, hc-Myc MOI=5, and hKlf4 MOI=3). Cells were incubated for 72 h at 37 °C with 5 % CO_2 and 20 % O_2. On day three post-transfection, cells were plated onto prepared 0.1 mg/mL Matrigel (Corning) coated plates in StemPro-34 Serum-Free Medium. The StemPro-34 Serum Free Medium was replaced with Essential 8 Medium (Thermofisher Scientific) on day eight post-transduction gradually over two days. Hereafter, daily Essential 8 medium replacement was done until individual pure hiPSC clones were manually selected and transferred to 0.1 mg/mL Matrigel-coated plates and maintained. Every 4 days, hiPSCs were passaged as clumps with 0.5 mM EDTA/PBS at a ratio of 1:3–1:12 in Essential 8 medium supplemented with 5 μM ROCK inhibitor Y27632 (Selleck Chemicals) at 37 °C with 5 % CO_2 and 20 % O_2.

3.2. Trilineage

Trilineage differentiation was performed using an Endoderm- (R and D Systems Cat# AF1924), mesoderm- (Santa Cruz, Cat# sc-374321), and ectoderm kit (R and D Systems Cat# AF1979). Germ layer specificity was confirmed with immunofluorescence microscopy (See section 3.4 *Immunofluorescence*) using germ layer-specific antibodies; SOX17 (Endoderm), Brachyury T (Mesoderm), OTX2 (Ectoderm) (Table 1).

3.3. Immunofluorescence

All hiPSC lines were checked between passages 14–20 and fixed in paraformaldehyde (4 %) for 15 min. Next, the hiPSCs were incubated with a blocking/permeabilization buffer (5 % BSA/0.3 % Triton-X-100 in PBS) for 30 min. After blocking with 1:5 diluted blocking buffer DPBS, the primary antibodies (Table 2) were added and incubated overnight at 4 °C. After washing with PBS, Alexa-conjugated secondary antibodies (Table 2) diluted in 1:5 diluted blocking/permeabilization buffer were incubated for one hour in the dark at room temperature. Cell nuclei were visualized using 0.5 μg/ml Hoechst or DAPI (Life Technologies, Thermo Fisher Scientific) before imaging using a Leica DMi8 confocal microscope (Pluripotency) or Nikon Ti2 Widefield microscope (Trilineage).

3.4. RNA isolation, cDNA synthesis, and qRT-PCR

RNA was extracted from hiPSCs (between passages 12–20) using TriPure (Sigma Aldrich) before cDNA synthesis using the iScript cDNA Synthesis Kit (Quatetect), both performed according to the manufacturer's instructions. cDNA was diluted 20 times with MilliQ, before adding SYBR Green Master Mix (Biorad). Relative gene expression of the pluripotency genes was determined by qRT-PCR using primers (Table 2) and a CFX96 Touch Real-Time PCR Detection System (Bio-Rad). qPCR reactions were run in duplicate (5 min. at 95 °C; 40 cycles of 30 s at 95 °C, 30 s at 60 °C and 30 s at 70 °C, followed by melting curve analysis). The ΔΔCt was determined by comparing it to the gene expression of TBP, subsequently, the relative fold increase in expression was calculated by 2ˆ-ΔΔCt.

3.5. Karyotyping

The karyotyping analysis was carried out by ddPCR (Stemgenomics), and with the ddPCR analysis of 24 Targeted hot spots. All hiPSC lines were checked between passages 18–25.

Table 1
Characterization and validation.

Classification	Test	Result	Data
Morphology	Photography Bright field	Normal	Fig. 1B
Phenotype	Qualitative analysis: Immunofluorescence	Positive for pluripotency markers TRA-1–60 and OCT4, SSEA and SO2	Fig. 1C
	Quantitative analysis: RT-qPCR	Expression of pluripotency genes (*OCT4, cMYC, KLF4, NANOG, ZFP42*) was assessed by qPCR	Fig. 1C
Genotype	Karyotype (ddPCR)	Normal; male; 46, XY or female; 46, XX.	Fig. S1A
Identity	Microsatellite PCR STR analysis	Not performed 17 loci analyzed, ruled out cross-contamination	N/A Available on request
Mutation analysis	Sanger Sequencing	Heterozygotic variant present in the patients and absent in the healthy proband	Fig. 1D
Microbiology and virology	Mycoplasma	MycoAlertTM Mycoplasma Detection Kit: All negative	Fig. S1B
Differentiation potential/List of recommended germ layer markers	Trilineage germ layer spontaneous differentiation	Immunofluorescence staining of SOX17 (endoderm), Brachyury T (mesoderm), and OTX2 (ectoderm)	Fig. 1E
Donor screening (OPTIONAL)	HIV 1 + 2 Hepatitis B, Hepatitis C	All negative	Not shown but available with author.
Genotype – additional info	Blood group genotyping		Not shown but available with author.
	HLA tissue typing		Not shown but available with author.

3.6. STR profiling

DNA was extracted from hiPSCs using the GeneJET Genomic DNA Purification Kit (Thermo Fisher Scientific) and sent to ACTT. STR analysis for seventeen STR loci plus the gender-determining locus was performed using the PowerPlex 18D Kit (Promega).

3.7. Sanger sequencing

Genomic DNA was extracted using the E.Z.N.A. Tissue DNA kit (Omega Bio-Tek). PCR was performed using a custom-designed primer pair for the *CRYAB* gene (Sigma-Aldrich; Table 2) following manufacturer's instructions. Thermal cycle program initiated with 3 min. at

Table 2
Reagents details. *RRID Requirement for antibodies*: use http://antibodyregistry.org/ to retrieve RRID for antibodies and include ID in table as shown in examples.

	Antibodies used for immunocytochemistry			
	Antibody	**Dilution**	**Company Cat #**	**RRID**
Pluripotency Markers	Mouse anti-OCT3/4	1:200	Santa Cruz, Cat# sc-5279	AB_628051
	Rat anti-SOX2	1:200	Thermo Fisher Scientific, # MA1-014	AB_2536667
	Mouse anti-SSEA IgG3	1:200	Thermo Fisher Scientific Cat# A24866,	AB_2651001
	Mouse anti-TRA-1–60 IgM	1:200	Thermo Fisher Scientific Cat# A24868	AB_2651002
Germ layer markers				
Endoderm	Goat anti-Human SOX17	1:10	R and D Systems Cat# AF1924	AB_355060
Ectoderm	Goat anti-Human Otx2	1:10	R and D Systems Cat# AF1979	AB_2157172
Mesoderm	Mouse anti-Brachyury T (A4)	1:300	Santa Cruz, Cat# sc-374321	AB_10990301
Secondary antibodies	Donkey anti-Rat Alexa Fluor 488	1:250	Thermo Fisher Scientific, Cat#A-21208	AB_141709
	Goat anti-Mouse IgG Alexa Fluor 488	1:200	Thermo Fisher Scientific, Cat#A11001	AB_2534069
	Donkey anti-Goat IgG Alexa Fluor 555	1:200	Invitrogen, Cat# A-21432	AB_2535853

	Primers		
	Target	**Size of band**	**Forward primer (5′-3′)/Reverse primer (5′-3′)**
Pluripotency markers (qRT-PCR)	SOX2	N/A	TGGACAGTTACGCGCACATCGAGTAGGACATGCTGTAGGT
	MYC	N/A	GCGAACCCAAGACCCAGGCCTGCTCCCAGGGGGTCTGCTCGCACCGTGATG
	NANOG	N/A	TGCAAGAACTCTCCAACATCCTATTGCTATTCTTCGGCCAGTT
	OCT4	N/A	AGGTGTTCAGCCAAACGACCTGATCGTTTGCCCTTCTGGC
	ZFP42	N/A	TAGAATGCGTCATAAGGGGTGATCTTGCCTGTCATGTACTCAGAA
	KLF4	N/A	CTGCGGCAAAACCTACACAAATTATCGTCGACCACTGTGCTGG
Housekeeping marker	TBP	N/A	TATAATCCCAAGCGGTTGCGCTGGAAAACCCAACTTCTG
Sanger Sequencing	CRYAB	N/A	GCAGCAGTCCTATTGTTCTGGAACACTCCATATCCGATTTAGTCACCGG

98 °C for degradation, followed by 35 cycles (with 1 °C degradation per cycle) of 10 s at 98 °C; 30 s at 66 °C, and 1 min. at 72 °C, and finished with a final extension of 5 min at 72 °C. DNA fragments were purified using the GeneJET purification protocol (Thermo Fisher Scientific) and 5 ng/μL per cell line was sent for sanger sequencing analysis via TubeSeq service of Eurofins Genomics.

3.8. Mycoplasma detection

All hiPSC lines were routinely checked every 2–4 months using the MycoAlert kit (Lonza).

CRediT authorship contribution statement

Ilse R. Kelters: Methodology, Resources, Writing – original draft, Writing – review & editing. **Devin Verbueken:** Methodology, Writing – review & editing. **Tess Beekink:** Investigation. **Linda W. Van Laake:** Writing – review & editing. **Joost P.G. Sluijter:** Writing – original draft, Writing – review & editing. **Renee G.C. Maas:** Conceptualization, Writing – original draft, Writing – review & editing. **Jan W. Buikema:** Conceptualization, Methodology, Writing – original draft, Writing – review & editing.

Declaration of competing interest

The authors declare that they have no known competing financial interests or personal relationships that could have appeared to influence the work reported in this paper.

Data availability

No data was used for the research described in the article.

Appendix A. Supplementary data

Supplementary data to this article can be found online at https://doi.org/10.1016/j.scr.2024.103497.

References

Alam, S., Abdullah, C.S., Aishwarya, R., Morshed, M., Nitu, S.S., Miriyala, S., Panchatcharam, M., Kevil, C.G., Orr, A.W., Bhuiyan, M.S., 2020. Dysfunctional mitochondrial dynamic and oxidative phosphorylation precedes cardiac dysfunction in R120G-αbcrystallin-induced desmin-related cardiomyopathy. J. Am. Heart Assoc. 9, 17195. https://doi.org/10.1161/JAHA.120.017195.

Cheng, L., Zou, X., Wang, J., Zhang, J., Mo, Z., Huang, H., 2023. The role of CRYAB in tumor prognosis and immune infiltration: A Pan-cancer analysis. Front. Surg. 9 https://doi.org/10.3389/FSURG.2022.1117307.

Marcos, A.T., Amorós, D., Muñoz-Cabello, B., Galán, F., Rivas Infante, E., Alcaraz-Mas, L., Navarro-Pando, J.M., 2020. A novel dominant mutation in CRYAB gene leading to a severe phenotype with childhood onset. Mol. Genet. Genomic Med. 8, 1290. https://doi.org/10.1002/MGG3.1290.

Mitra, A., Basak, T., Datta, K., Naskar, S., Sengupta, S., Sarkar, S., 2013. Role of α-crystallin B as a regulatory switch in modulating cardiomyocyte apoptosis by mitochondria or endoplasmic reticulum during cardiac hypertrophy and myocardial infarction. Cell Death Dis. 4 https://doi.org/10.1038/CDDIS.2013.114.

Van der Smagt, J.J., Vink, A., Kirkels, J.H., Nelen, M., ter Heide, H., Molenschot, M.M.C., Weger, R.A., Schellekens, P.A.W., Hoogendijk, J., Dooijes, D., 2014. Congenital posterior pole cataract and adult onset dilating cardiomyopathy: expanding the phenotype of αB-crystallinopathies. Clin. Genet. 85, 381–385. https://doi.org/10.1111/CGE.12169.